A Global Approach for Least-Squares Image Matching and Surface Reconstruction in Object Space

Christian Heipke
Chair for Photogrammetry and Remote Sensing, Technical University Munich, Arcisstr. 21, D-8000 Munich 2, Federal Republic of Germany

ABSTRACT: The automatic determination of corresponding points in digital images, called "digital image matching," is one of the key factors limiting complete automation in photogrammetry. In recent research work at different institutions a tendency has been observed for performing digital image matching on a global scale and in object space. In view of these facts, a general model for digital photogrammetry, developed over the last three years and integrating area-based multi-image matching, point determination, object surface reconstruction, and orthophoto generation into one model only, is presented in this paper. In a least-squares adjustment, the unknown quantities (geometric and radiometric parameters of the object surface, and orientation parameters of the images) are iteratively estimated from pixel intensity values and control information. Simulated and practical examples demonstrate the possibilities of the approach. The radius of convergence (pull-in range), known to be rather small in least-squares image matching, is considerably extended, and the computation time is drastically reduced when using a hierarchical procedure (image pyramids). If more than two images are used, the approach has been found to be robust against certain disturbances in the intensity distribution of the images.

INTRODUCTION

ONE OF THE MAIN DIFFICULTIES in digital photogrammetry is that of the automatic measurement of image coordinates of corresponding points for the computation of object space coordinates. This problem is referred to as "image matching."

Because no unified theory of human stereo vision exists to date, a large number of more or less heuristic algorithms for image matching have been proposed over the years (for excellent surveys see Barnard and Fischler (1982), Lemmens (1988), and Wrobel (1988)).

The two main research directions are area-based and feature-based image matching. Whereas in the first method the image intensity values of different images are matched directly, in the second method features (points, edges, lines) are extracted separately from the images and are matched in a further step.

In digital photogrammetry much attention has been paid to area-based matching, in particular to least-squares methods, since they were first introduced (Helava, 1976; Wild, 1979; Pertl and Ackermann, 1982; Förstner, 1982), mainly for three reasons:

- extremely high accuracy potential,
- high degree of invariance against geometric image distortions, and
- relatively simple possibilities for statistical analysis of the results.

Various extensions of the original idea can be found for instance in Grün (1985) and Rosenholm (1986).

Also, it became clear, that isolated matching of small image windows can be subject to blunders, especially in areas of poor or repetitive image texture, or when the object surface shows discontinuities. Therefore, research in area-based image matching has shifted to global approaches and is more and more performed in object space (Rosenholm, 1986; Barnard, 1987; Hoff and Ahuja, 1989; Chernuschi-Frias et al., 1989). In this approach the reflectance properties of the object surface and the scene illumination can also be taken into account.

In this paper, a global object-based multi-photo approach is investigated. It integrates area-based image matching, point determination, object-surface reconstruction, and orthophoto generation into a single model. The unknown quantities (radiometric and geometric parameters for the approximation of the object surface and the orientation parameters of the images) are estimated directly from the pixel intensity values and control information in a least-squares adjustment. Any desired number of images, scanned in various spectral bands, can be processed simultaneously.

The next section gives a brief description of the approach. More details can be found in previous publications (Ebner *et al.*, 1987; Ebner and Heipke, 1988; Heipke, 1989; Heipke, 1990). In the third section results using simulated and real image data are presented. The last section discusses the advantages and the limitations of the approach and gives an outlook for future work.

Similar concepts have been developed independently at the Technical University Darmstadt (Wrobel, 1987) and at Helava Associates Incorporated (Helava, 1988). They are also currently under investigation at the Swedish Space Agency (Rosenholm, 1988), Volkswagen AG, Wolfsburg (Schneider, 1989), Stuttgart University (Ackermann and Zheng, 1990), and the Center for Space and Remote Sensing Research in Taiwan (Wu and Chang, 1990).

DESCRIPTION OF THE APPROACH

IMAGE FORMATION

In the following the process of image formation is explained, as much as is necessary for image matching. The selection of imaging parameters which influence the intensity value of a pixel is investigated. Further details can be found for instance in Horn (1986).

The intensity value of an image pixel depends mainly on the following four parameter groups:

- sensor and camera parameters (sensitivity to electromagnetic radiation, degree of transmission of the optics, etc.),
- atmospheric parameters (degree of atmospheric transmission between camera and object surface),
- object surface parameters (reflectance function),
- illumination parameters (number, direction, and brightness of illumination sources).

In order to keep the image formation model simple, only the

PHOTOGRAMMETRIC ENGINEERING & REMOTE SENSING,
Vol. 58, No. 3, March 1992, pp. 317–323.

0099-1112/92/5803-317$03.00/0

object surface parameters will be considered in the following. The other three parameter groups are assumed to be constant for the time interval between the image recordings. It is assumed that the object surface O can be represented by three-dimensional cartesian coordinates X, Y, Z relative to some reference plane (the XY plane is chosen here): that is,

$$O = O[X,Y,Z(X,Y)]. \quad (1)$$

The reflectance function R of the object surface depends on the position X,Y,Z, and, at this position, on the directions towards the light source b, the surface normal $\mathbf{n}$, and the viewing direction v:

$$R = R[X,Y,Z(X,Y), b, \mathbf{n}, v]. \quad (2)$$

$\mathbf{n}$ can be expressed in terms of the three cartesian coordinates

$$\mathbf{n}^T = [-dZ/dX \quad -dZ/dY \quad 1]. \quad (3)$$

In the following, perfect Lambertian reflection is assumed for the object surface. Therefore, R is independent of v. In the case of constant illumination parameters also b can be left out of consideration. Equation 2 can therefore be written as

$$R = R\,[X,Y,Z(X,Y)]. \quad (4)$$

Because these assumptions are not rigerously met in the imaging process, a radiometric image transformation T_r is introduced to compensate at least partially for the deviations. This simplification does not hold in general, but all image matching algorithms without prior knowledge about the object surface reflectance properties are faced with the same problem.

Thus, the relation between the reflectance function R and the image intensity value d, given in pixel space, can be written as

$$R\,[X,Y,Z(X,Y)] = T_r\,(d) \quad (5)$$

From Equation 5 the basic correspondence condition for the matching process can be derived: That is, the image intensity values of all corresponding points must be equal after applying the radiometric image transformation. Using the abbreviation $g = T_r(d)$, this can be expressed as

$$R\,[X,Y,Z(X,Y)] = g_i = \text{constant}; \; i = 1, \ldots, s \quad (6)$$

where s stands for the number of the given images.

Object Space Models

In this paragraph a geometric and a radiometric model in object space are introduced.

In the geometric model the object surface is assumed to be piecewise smooth. Thus, neighboring surface points are not independent from each other. This fact can be taken into account using the regularization theory (Tikhonov, 1963; Poggio, 1985) or by introducing the concept of finite elements (Ebner *et al.*, 1980). The latter has had much success in the field of digital terrain model (DTM) generation and is therefore chosen here.

In the XY plane of the object surface, a grid is defined with grid nodes X_k,Y_l and independent grid heights $Z(X_k,Y_l)$. The mesh size depends on the roughness of the terrain. A height $Z(X,Y)$ at an arbitrary point can then be interpolated from the neighboring grid heights.

As in digital terrain modeling (see, for example, Ebner *et al.* (1988)), the geometric model can be improved by introducing a variable grid size, break lines, and conditions for slope and curvature of the surface, if prior knowledge (e.g., location of break lines) concerning the object surface exists, or if this knowledge can be extracted from the images.

In the radiometric model, object surface elements of constant size are defined within each grid mesh. The size is chosen approximately equal to the pixel size multiplied by the image scale factor. A constant object intensity value $G(X,Y)$ is assigned to each object surface element. $G(X,Y)$ can be regarded as an orthophoto pixel of the terrain. The relation between $G(X,Y)$ and the reflectance function $R[X,Y,Z(X,Y)]$ will be given below.

The combination of the geometric and the radiometric model can be seen in Figure 1.

Least-Squares Adjustment

The object-surface elements can be projected into the different images using the well-known collinearity equations. Subsequently, image intensity values at the corresponding locations in pixel space can be resampled from the original pixel intensity values. The necessary transformations from object into pixel space involve four main steps (see Figure 2):

- for each object surface element, an elevation is computed from the neighboring grid heights $Z(X_k,Y_l)$, e.g., by bilinear interpolation;
- from the X,Y,Z coordinates of the center of an object surface element, image coordinates x_i, y_i can be derived using the collinearity equations;
- x_i, y_i are mapped into pixel space using a planar transformation (normally an affine transformation), yielding a position x_p, y_p; and
- because x_p, y_p are non-integer coordinates, the corresponding image intensity values $d(x_p,y_p)$ must be resampled from the original image data.

For T_r, a linear transformation is assumed to hold. In this case, T_r describes brightness and contrast differences between

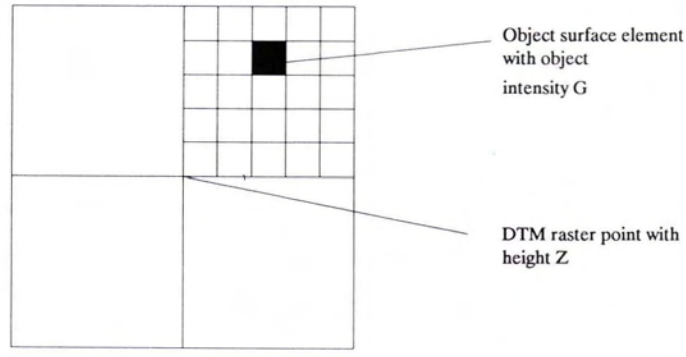

FIG. 1. Geometric and radiometric models in the XY plane of object space.

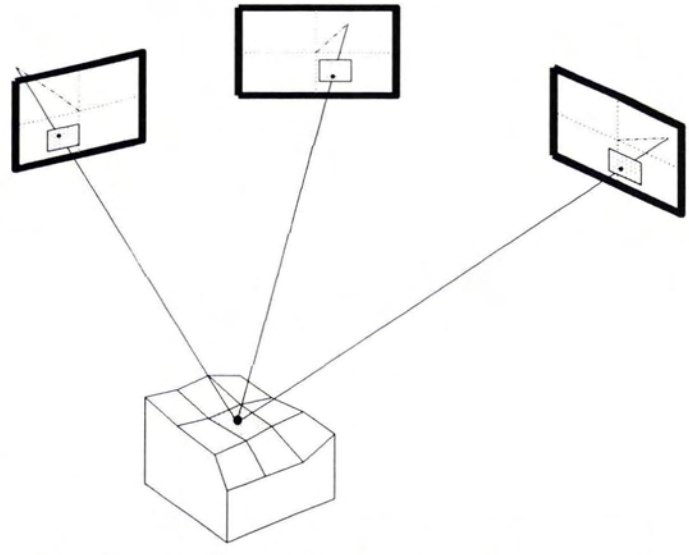

FIG. 2. Transformation of object surface elements into the images.

the images. One of the images (called image 1) is taken as reference and $T_{r,1}$ is consequently set constant. Therefore, the image intensity values d are not directly related to the reflectance function $R[X,Y,Z(X,Y)]$, but to $G(X,Y)$. The relation between R and G is given by

$$R[X,Y,Z(X,Y)] = T_{r,1}\,[G(X,Y)] \tag{7}$$

In the following, the grid heights $Z(X_k,Y_l)$, the parameters p for the exterior orientation of the images, the intensity values $G(X,Y)$ of the object surface elements, and the parameters of the radiometric transformation T_r (for all images but image 1) are treated as unknowns. They are estimated directly from the observations $d(x_p,y_p)$ and control information in a least-squares adjustment. Thus, $d(x_p,y_p)$ depends on the $Z(X_k,Y_l)$ and on p. For each object surface element, as many values $d(x_p,y_p)$ can be computed as there are images, and as many observation equations of the following type can be formulated (dropping the indices for the grid heights):

$$v = G - T_r[d(x_p(Z,p),y_p(Z,p))] \tag{8}$$

where

v	=	residual of observation equation
G	=	unknown intensity value of the object surface element
Z	=	unknown heights of the surrounding grid points
p	=	unknown parameters for the image orientations
$d(x_p,y_p)$	=	resampled image intensity value
T_r	=	radiometric transformation

The system of observation equations is completed by introducing control information with appropriate standard deviations. In the most simple case the weight matrix for the intensity value observations is represented by the identity matrix. Because the observation equations are nonlinear in Z and p, the solution of the least-squares adjustment is found iteratively.

APPLICATIONS

In this section two applications from aerial and industrial photogrammetry, respectively, are presented.

In the first case, the approach was applied to simulated image data with a realistic intensity value distribution. The investigations reported in this paper are concerned with the use of image pyramids to extend the radius of convergence, which is known to be rather small in least-squares image matching (a few pixels only).

In the second case, real imagery from réseau cameras was used. The camera réseau crosses appear in the images in different (non-corresponding) places. A digital surface model (DSM) was derived, and the effects of the réseau crosses on the matching results was investigated.

Test with Simulated Imagery

Image Material.

A black-and-white aerial photograph (image scale about 1:30.000, flying height about 4500 m) was scanned at the Bayerisches Landesvermessungsamt München with a Hell CTX 330 Scanner. The pixel size was 25 μm, corresponding to approximately 0.75 m at the ground, and the depth per pixel was 7 bits (which is the maximum intensity value resolution of this particular scanner).

In object space, a 20-m grid was defined, each mesh containing 20 by 20 object surface elements. Thus, the size of one pixel at ground level approximately corresponds to the size of an object surface element.

The relationship between the scanning coordinate system and the object coordinate system was established by an affine transformation and predefined orientation parameters for the image.

Using an existing DTM of 16 by 16 grid meshes, intensity values were assigned to the object surface elements by orthophoto projection (pixel-by-pixel method (Mayr and Heipke, 1988)).

This orthophoto was projected back into image space using four different sets of affine and orientation parameters. In each of the resultant images a pixel matrix of intensity values with 25-μm pixel size was derived by nearest neighbor interpolation and a filling algorithm where necessary. Thus, four simulated images were generated forming two stereo models, one in each of two crossing flight paths at an angle of approximately 40 degrees, with a longitudinal overlap of 60 percent and a scale of about 1:30.000.

The difference from real image data is that there is no influence from possibly wrong orientation parameters and from different photographs (involving occlusion, image noise, different light reflection, etc.).

The four simulated images superimposed with the borders of the matched areas can be seen in Figure 3.

The Test.

In theoretical and practical investigations it has been shown that the radius of convergence of least-squares image matching lies in the range of a few pixels only (Burkhardt and Moll, 1979; Grün and Baltsavias, 1988). Hierarchical matching procedures, namely the use of image pyramids (Burt and Adelson, 1983; Rosenfeld, 1984; Kropatsch, 1985), have the potential to extend this radius of convergence, provided that enough texture can be found in the images at each pyramid level. Also, the computations are sped up because in the upper pyramid levels fewer pixels have to be processed, and fewer iterations have to be performed in each pyramid level. The idea of a hierarchical procedure for image matching is not new at all (Sharp *et al.*, 1965). It has recently been applied by various authors (see, e.g., Baltsavias, 1988; Hannah, 1988; Hahn, 1989; El Hakim, 1989; Li, 1989). A further extension of using hierarchy consists in matching through scale space (Witkin *et al.*, 1987; Hahn, 1990).

The image pyramids for this test were derived by low-pass filtering of the original images and retaining only every second pixel in the row and column direction for the next level. Thus, the image in a level of the pyramid contains four times less

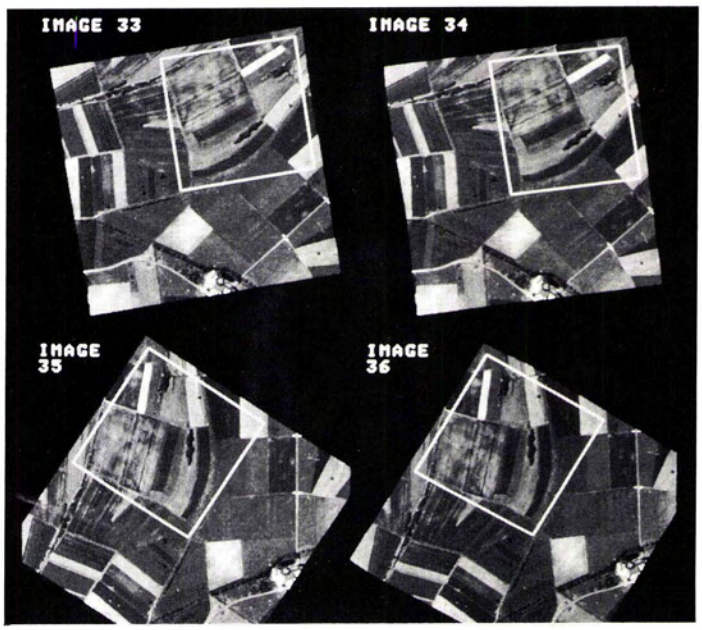

FIG. 3. The four simulated images superimposed with the matched area.

pixels than the image in the level one below. The image pyramid for one of the images is shown in Figure 4. It consists of the levels 0 to 3.

For the matching procedure the DTM with 16 by 16 grid meshes, which was used for the generation of the simulated images, was taken as reference. The orientation parameters of the images were held constant. Thus, no control information was necessary. The computations were terminated when the height change from one iteration to the next fell below a predefined threshold (0.1 m, corresponding to a mean displacement of 0.04 pixels in the images) at each grid point.

The initial values for the grid heights were varied in two different ways. A constant shift corresponding to a displacement of four pixels in image space was applied to all grid heights of the reference DTM (labeled CON 4), and a random generator was used to produce height shifts with mean zero and a predefined standard deviation also corresponding to four pixels in image space (labeled SIG 4).

Using these heights as initial values, the matching procedure was run twice: once on the original images only and once through the four levels of the image pyramid. To ensure that in every pyramid level the same number of pixels per DTM grid mesh was used (namely, 20 by 20), the size of the DTM grid meshes had to be multiplied by four from level to level. Thus, in level 3, only 2 by 2 grid meshes were matched; in level 2 and 1, 4 by 4 and 8 by 8 grid meshes, respectively, were matched; and only at level 0 was the original number of 16 by 16 grid meshes matched. The results of one level were always used as initial values for the next lower level.

The results of the test are given in Table 1. The number of necessary iterations, the theoretical standard deviations for the grid heights (more or less constant for all grid points), the empirical standard deviations of the grid heights as computed from the reference DTM, and the maximum difference from the reference DTM are shown. The grid heights at the border of the DTM have been found to be less reliable because they are not stabilized by the geometric model in the same way as the heights in the interior. Therefore, the two outermost border heights were left out of consideration for the calculation of the differences between the computed results and the reference DTM.

The following conclusions can be drawn from Table 1:

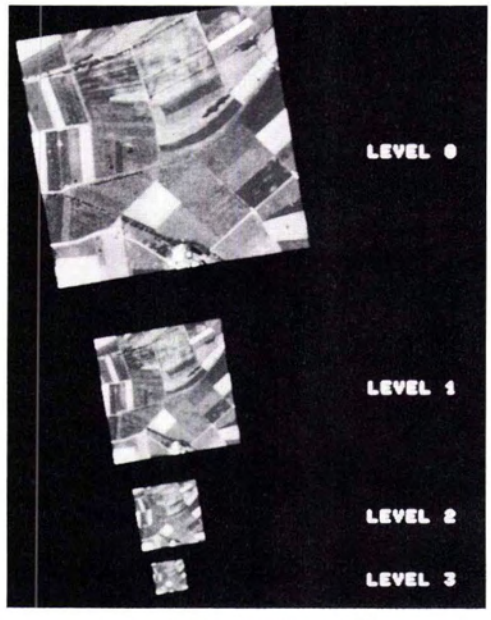

FIG. 4. The image pyramid.

- using the original images, the radius of convergence is smaller than four pixels and the computations are stopped after very many iterations, yielding wrong results (large empirical standard deviation and large maximum difference);
- the radius of convergence is enlarged when the matching procedure is run through the image pyramids, and the results are correct in this case;
- the theoretical standard deviations of the grid heights are proportional to the pixel size (for a theoretical explanation see Förstner (1984));
- the computation time is drastically reduced using the image pyramids. For CON 4 and SIG 4, instead of 189 and 65 iterations, only 21 are necessary, only seven of which have to be performed on the lowest, computationally most expensive, level; and
- the results for CON 4 and SIG 4 in the image pyramids are similar.

TEST WITH REAL IMAGERY

Image Material.

For this investigation, image data from industrial photogrammetry were chosen. They were obtained from the Volkswagen AG, Wolfsburg within a project in cooperation with the Technical Universities of Braunschweig, Darmstadt, and Munich. The aim of the project is a dense description of a car body surface with an accuracy of better than 0.1 mm. This description can then be used as reference for further design and in the production process, and for documentation purposes. Four convergent analog images of a car part, superimposed with a random dot texture as used in the Zeiss InduSURF system (Claus, 1987), were taken with Rolleiflex 6006 réseau cameras (see Figure 5). They are numbered 25, 468, 45, and 143 consecutively.

The orientation parameters of the images were calculated in a bundle adjustment using six control points and 21 tie points in the four images.

One small square in each image with tie point no. 108 in the center was digitized with the Rollei CCD réseau scanner (Luhmann, 1988). Each region (see Figure 6) consists of 512 by 512 pixels at an effective intensity resolution of 6 bits. The pixel size was 8 μm by 5 μm, and the image scale in the digitized regions amounts to approximately 1:20. The parameters for the transformation from image to scanning coordinates are provided by the scanner software.

The image data are of rather poor radiometric quality. In some parts no intensity gradients are present. Image 143 shows a camera réseau cross in the center, while images 468 and 45 show one at the border of the digitized square (see Figure 6). According to the principles of réseau cameras, these réseau crosses appear in non-corresponding locations. Therefore, they constitute disturbances in the intensity value distribution, comparable

TABLE 1. MATCHING RESULTS USING THE ORIGINAL IMAGERY AND THE IMAGE PYRAMID

		CON 4	SIG 4
Matching on level 0 only:			
Number of iterations		189	65
Theor. stand. dev. of heights [m]		0.05	0.05
Empir. stand. dev. of heights [m]		0.24	0.12
Max. difference to reference [m]		3.19	1.58
Pyramid matching:			
Level 3	Number of interations	4	4
	Theor. stand. dev. of heights [m]	0.4	0.4
Level 2	Number of iterations	5	5
	Theor. stand. dev. of heights [m]	0.2	0.2
Level 1	Number of iterations	5	5
	Theor. stand. dev. of heights [m]	0.1	0.1
Level 0	Number of iterations	7	7
	Theor. stand. dev. of heights [m]	0.05	0.05
	Empir. stand. dev. of heights [m]	0.04	0.04
	Max. difference to reference [m]	0.27	0.27

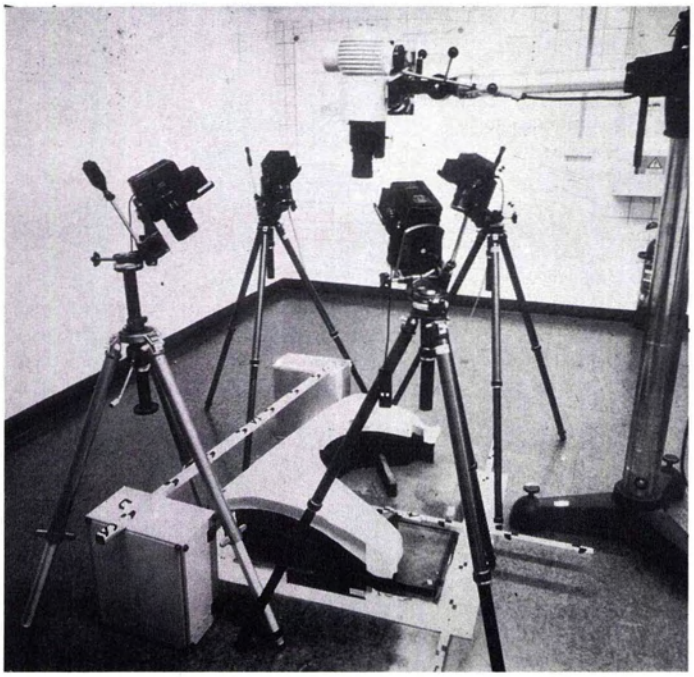

FIG. 5. Acquisition of the analog images.

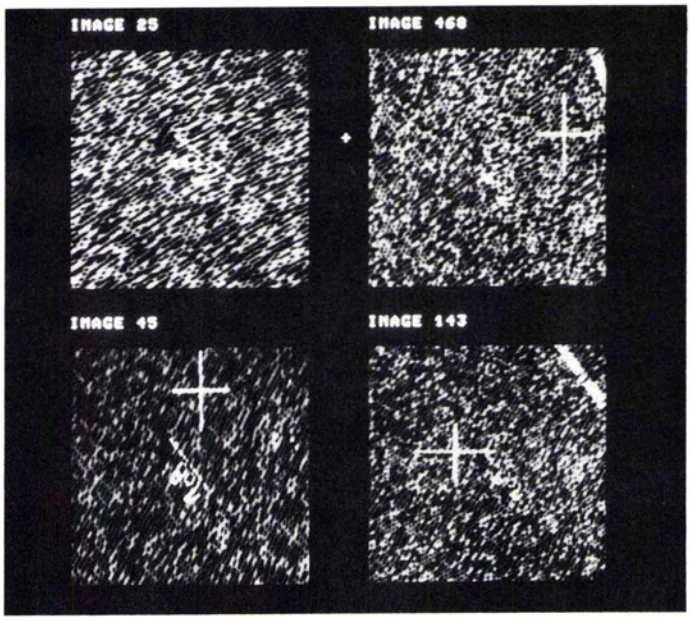

FIG. 6. The four digitized image regions.

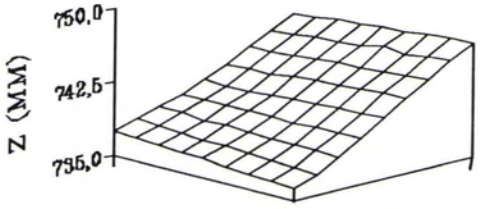

FIG. 7. DSM generated from all three images.

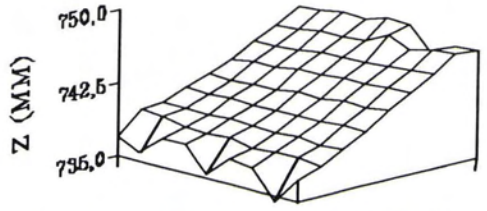

FIG. 8. DSM generated from images 25 and 45.

to the specular reflection properties of the object surface. It was decided to leave out image 143 and to use only images 25, 468, and 45 for the test. Because the réseau cross in image 468 does not lie in the matched area, whereas the one in image 45 does, the matching of images 25 and 468 is expected to yield correct results. The effect of the réseau cross in image 45 on the results can thus be investigated.

The test.

The aim of this test was to derive a digital surface model (DSM) for the car part from the three images and to study the effects of the réseau cross in image 45. Because reference data were not available and could not be measured with sufficient accuracy by means of analytical photogrammetry (Heipke, 1990), no external accuracy can be given for the results.

In object space, a DSM grid with 10 by 10 grid meshes and 3-mm grid size was defined. Each DSM grid mesh was to contain 20 by 20 object surface elements. Because an approximate height value was given only for tie point 108, an iterative algorithm, described earlier (Heipke, 1989), had to be used to provide initial values for all grid points.

The orientation parameters were held fixed for the DSM derivation. The computations were terminated when the height change from one iteration to the next fell below a predefined threshold (20 μm in the middle of the DSM, 60 μm at the border) at each grid point. Two different values were used because the border heights are less reliable (see above).

The resultant DSM from all three images is shown in Figure 7 (the border heights are not plotted). It can be seen that the slope of the surface is rather constant, and consequently the curvature is very small. The camera réseau cross in image 45 does not disturb the results. This could be shown by comparing the DSM to the one generated from the error-free images 25 and 468 only.

In Figure 8 the DSM derived from images 25 and 45 is depicted. As was to be expected, the result is incorrect. The reason is that the camera réseau cross in image 45 caused disturbances of the DSM in the upper part. Besides, errors also occur in the lower part of the DSM. No explanation can be given for the latter errors.

The main result of this test is the fact that the matching procedure is capable of handling certain observations in image space, which are not consistent with the used model (e.g., the camera réseau cross in image 45), and still yields correct results, provided that more than two images are present. Three reasons can be given to explain this behavior:

- the object surface is stabilized by the geometric model,
- the intensity values of the two other images are sufficient for a correct derivation of the DSM, and
- not all observations of the grid meshes containing the réseau cross in image 45 are incorrect.

DISCUSSION OF THE APPROACH AND OUTLOOK

The described approach forms a very general model of digital photogrammetry for all tasks not involving feature or semantic

information extraction. Because in the digital domain points are represented by small areas, point determination can be formulated as a special case of this approach. Also, orthophoto projection is part of the process because the intensity values $G(X,Y)$ of the object surface elements can be regarded as pixels of an orthophoto of the terrain (although it must be mentioned that this orthophoto differs from conventional orthophotos in that each $G(X,Y)$ is computed from various images instead of from one image only).

All methods used in analytical photogrammetry (e.g., combined point determination including self calibration of the cameras or processing of line sensor imagery) can be integrated into this approach. The possible use of a complex radiometric transformation allows for the introduction of knowledge about the reflectance properties of the object surface and the illumination sources. Therefore, this method can be regarded as a base for many computer vision approaches, including shape-from-shading or shape-from-texture to name only a few (Wrobel, 1989; Weisensee, 1990).

The theoretical limitations of the approach can be divided into geometric and radiometric limitations according to the different models in object space.

The object surface is assumed to be continuous. Therefore, images of objects like the Eiffel tower in Paris, a railway steel bridge, or a building crane cannot be processed. In addition, only one value $Z(X,Y)$ is allowed for each object surface element. Thus, vertical surfaces can only be handled by rotating the object coordinate system.

Radiometric limitations (common for nearly all image matching methods) come from the necessity of sufficient image texture (in all frequencies, if a hierarchical procedure is used). It is, however, possible to bridge small areas of poor image texture because of the global formulation of image matching (Heipke, 1990).

Furthermore, the object surface must be opaque (otherwise the recorded image intensity value would result from light reflected at different object surface elements), and specular reflection is not allowed.

For the practical applicability of the method, critically assessed by Helava (1988), the necessary quality of the initial values for the unknowns in the adjustment, the computational speed, and the reliability of the results are the main issues which have to be considered.

These three points have been dealt with in this paper. The radius of convergence and the computational speed are improved using hierarchical matching procedures (image pyramids), as long as enough texture is available on each level. As for the computing time, further accelerations are necessarry, however. A parallel version of the presented method may solve this problem.

Reliability is a key problem in digital image matching because many gross errors can occur in the matching procedure due to the radiometric limitations mentioned above. In addition, the number of pixels processed simultaneously is extremely high, so checking becomes a very time consuming task. In this example it could be shown that observations, not consistent with the adjustment model, in certain cases do not effect the results if more than two images are processed simultaneously. These inconsistencies can come from camera réseau crosses, but also from occlusions, shadows, or anisotropic light reflection at the object surface.

Further work is needed to explicitly model these inconsistencies by intelligent preprocessing of the imagery (e.g., recognition of shadows and exclusion of the corresponding area from the matching) and by improving the geometric model of the object surface. Automatically finding and introducing break lines (Kölbl and da Silva, 1988; Li, 1989) or height discontinuities (Blake and Zisserman, 1987; Zheng and Hahn, 1990) is a promising way for improving the geometric model.

Another point, which should be investigated in more detail, is the human interface. Because fully automatic DTM generation will only be feasible for special applications in the near future, human interaction will be necessary. Questions arise: How can the matching procedure best be incorporated into a digital photogrammetric system? What are the best algorithms for a reliable automatic check of the results? How can the matching results best be visualized for interactive control?

Other problems not yet mentioned comprise the use of multispectral, multiresolution, multisensor, and multitemporal imagery. Also, experimental investigations on using complex radiometric transformations still have to be carried out. Thus, digital image matching still remains a major field of research.

REFERENCES

Ackermann, F., and Y. Z. Zheng, 1990. Inverse and ill-posed problems in photogrammetric surface reconstruction, *International Archives of Photogrammetry and Remote Sensing*, Symposium Wuhan, Com. III, Vol. 28, Part 3, pp. 22–47.

Baltsavias, E., 1988. Hierarchical multiphoto matching and DTM generation, *International Archives of Photogrammetry and Remote Sensing*, Congress Kyoto, Commission III, Vol. 27, Part B11, pp. 115–130.

Barnard, S. T., 1987. *Stereo Matching by Hierarchical Microcanonical Annealing*, SRI International, Technical Note 414.

Barnard, S. T., and M. A. Fischler, 1982. Computational stereo, Association for Computing Machinery, *Computing Surveys*, Vol. 14, No. 4, pp. 553–571.

Blake, A., and A. Zisserman, 1987. *Visual Reconstruction*, The MIT Press, Cambridge, Massachussetts.

Burkhardt, H., and H. Moll, 1979. A modified Newton-Raphson search for the model-adaptive identification of delays, 5. *IFAC Symposium on Identification and System Parameter Estimation*, Darmstadt, pp. 1279–1286.

Burt, P. J., and E. H. Adelson, 1983. The Laplacian pyramid as a compact image code, *IEEE-Transactions on Communications* Vol. 31, No. 4, pp. 532–540.

Chernuschi-Frias, B., D. B. Cooper, Y. P. Hung, and P. N. Belhumeur, 1989. Toward a model-based Bayesian theory for estimating and recognizing parameterized 3-D objects using two or more images taken from different positions, *IEEE-PAMI* Vol. 11, No. 10, pp. 1028–1052.

Claus, M., 1987. Automatische, photogrammetrische Oberflächenvermessung von Industrieprodukten, *Verein Deutscher Ingenieure-Berichte*, No. 659, pp. 241–250.

Ebner, H., D. Fritsch, W. Gillessen, and C. Heipke, 1987. Integration von Bildzuordnung und Objektrekonstruktion innerhalb der digitalen Photogrammetrie, *Bildmessung und Luftbildwesen* Vol. 55, No. 5, pp. 194–203.

Ebner H., and C. Heipke, 1988: Integration of digital image matching and object surface reconstruction, *International Archives of Photogrammetry and Remote Sensing*, Congress Kyoto, Commission III, Vol. 27, Part B11, pp.III-534–545.

Ebner, H., B. Hofmann-Wellenhof, P. Reiβ, and F. Steidler, 1980. HIFI - A minicomputer program package for height interpolation by finite elements, *International Archives of Photogrammetry and Remote Sensing*, Congress Hamburg, Commission IV, Vol. 23, Part B4, pp. 202–215.

Ebner, H., W. Reinhardt, and R. Höβler, 1988. Generation, management, and utilization of high fidelity digital terrain models, *International Archives of Photogrammetry and Remote Sensing*, Congress Kyoto, Commission III, Vol. 27, Part B11, pp. III-556–566.

El-Hakim, S. F., 1989. A hierarchical approach to stereo vision, *Photogrammetric Engineering & Remote Sensing*, Vol. 55, No. 4, pp. 443–448.

Förstner, W., 1982. On the geometric precision of digital correlation, *International Archives of Photogrammetry and Remote Sensing*, Symposium Helsinki, Commission III; Vol. 24, Part 3, pp. 176–189.

———, 1984. Quality assessment of object location and point transfer using digital image correlation techniques, *International Archives of Photogrammetry and Remote Sensing*, Congress Rio de Janeiro, Commission III, Vol. 25, Part A3, pp. 197–219.

Grün, A., 1985. Adaptive least squares correlation: A powerful image matching technique, *South African Journal of Photogrammetry, Remote Sensing and Cartography* Vol. 14, No. 3, pp. 175–187.

Grün, A., and E. Baltsavias, 1988. Geometrically constrained multiphoto matching, *Photogrammetric Engineering & Remote Sensing*, Vol. 54, No. 5, pp. 633–641.

Hahn, M., 1989. Automatic measurement of digital terrain models by means of image matching techniques, *Schriftenreihe des Instituts für Photogrammetrie der Universität Stuttgart*, Heft 13, pp. 141–152.

———, 1990. Estimation of the width of the point-spread function within image matching, *International Archives of Photogrammetry and Remote Sensing*, Symposium Wuhan, Com. III, Vol. 28, Part 3, pp. 246–267.

Hannah, M. J., 1988. Digital stereo image matching techniques, *International Archives of Photogrammetry and Remote Sensing*, Congress Kyoto, Commission III, Vol. 27, Part B3, pp. 280–293.

Heipke, C., 1989. An integral approach to digital image matching and object surface reconstruction, *Optical 3-D Measurement Techniques* (A. Grün and H. Kahmen, editors), Wichmann Verlag, Karlsruhe, pp. 347–359.

———, 1990. *Integration von digitaler Bildzuordnung, Punktbestimmung, Oberflächenrekonstruktion und Orthoprojektion in der digitalen Photogrammetrie*, Deutsche Geodätische Kommission, Reihe C, No. 366.

Helava, U. V., 1976. Digital correlation in Photogrammetric Instruments, *International Archives of Photogrammetry and Remote Sensing*, Congress Helsinki, Com. II, Vol. 21.

———, 1988. Object-space least-squares correlation, *Photogrammetric Engineering & Remote Sensing*, Vol. 54, No. 6, pp. 711–714.

Hoff, W., and N. Ahuja, 1989. Surface from stereo: Integrating feature matching, disparity, estimation, and contour detection, *IEEE-PAMI* Vol. 11, No. 2, pp. 121–136.

Horn, B. K. P., 1986. *Robot Vision*, The MIT Press, Cambridge, Massachussetts.

Kölbl, O., and I. da Silva, 1988. Derivation of a digital terrain model by dynamic programming, *International Archives of Photogrammetry and Remote Sensing*, Congress Kyoto, Commission III, Vol.27, Part B8, pp. 77–86.

Kropatsch, W. G., 1985. A pyramid that grows by powers of two, *Pattern Recognition Letters* Vol. 3, pp. 315–322.

Lemmens, M., 1988. A survey on stereo matching techniques, *International Archives of Photogrammetry and Remote Sensing*, Congress Kyoto, Commission V, Vol. 27, Part B8, pp. 11–23.

Li, M., 1989. *Detection and Location of Breaklines and Discontinuities in Stereo Image Matching*, Phot. Reports No. 54, Royal Institute of Technology, Stockholm.

Luhmann, T., 1988. *Ein hochauflösendes automatisches Bildmeßsystem*, Wissenschaftliche Arbeiten der Universität Hannover, No. 154.

Mayr, W., and C. Heipke, 1988. A contribution to digital orthophoto generation, *International Archives of Photogrammetry and Remote Sensing*, Congress Kyoto, Commission IV, Vol. 27, Part B11, pp. IV-430–439.

Pertl, A., and F. Ackermann, 1982. Zuordnung kleiner Bildflächen durch digitale Korrelation, *Bericht für das Kolloqium im DFG Schwerpunktprogramm "Fernerkundung"*.

Poggio, T., 1985. Early vision: From computational structure to algorithms and parallel hardware, *Computer Vision, Graphics, and Image Processing* Vol. 31, pp. 139–155.

Rosenfeld, A. (ed.), 1984. *Multiresolution Image Processing and Analysis*, Springer Verlag, Berlin.

Rosenholm, D., 1986. Accuracy improvement of digital matching for evaluation of digital terrain models, *International Archives of Photogrammetry and Remote Sensing*, Symposium Rovaniemi, Commission III, Vol. 26, Part 3/2, pp. 573–587.

———, 1988. Multi-point matching along vertical lines in SPOT images, *International Journal of Remote Sensing*, Vol. 9, Nos. 10-11, pp. 1687–1703.

Schneider, C. T., 1989. Optische Oberflächenvermessung auf der Basis von objektgestützter Mehrbildzuordnung, *Optical 3-D Measurement Techniques* (A. Grün and H. Kahmen, editors), Wichmann Verlag Karlsruhe, pp. 370–379.

Sharp, J. V., R. L. Christensen, W. L. Gilman, and F. D. Schulman, 1965. Automatic map compilation using digital techniques, *Photogrammetric Engineering & Remote Sensing* Vol. 31, No. 3, pp. 223–239.

Tikhonov, A. N., 1963. Solution of incorrectly formulated problems and the regularization method, *Soviet Mathematical Dokl.* Vol. 4, pp. 1035–1038.

Weisensee, M., 1990. Fundamentals of shape from X techniques, *International Archives of Photogrammetry and Remote Sensing*, Symposium Wuhan, Com. III, Vol. 28, Part 3, pp. 985–999.

Wild, E., 1979. Interner Bericht, Universität Stuttgart.

Witkin, A., D. Terzopoulos, and M. Kass, 1987. Signal matching through scale space, *International Journal of Computer Vision*, Vol. 1, pp. 133–144.

Wrobel, B., 1987. Facets stereo vision (FAST Vision) - A new approach to computer stereo vision and to digital photogrammetry, *Interlaken, Proc. Fast Processing of Photogrammetric Data*, pp. 231–258.

———, 1988. Least squares methods for surface reconstruction from images, *International Archives of Photogrammetry and Remote Sensing*, Congress Kyoto, Commission III, Vol. 27, Part B3, pp. 806–821.

———, 1989. Geometrisch-physikalische Grundlagen der digitalen Bildmessung, *Schriftenreihe des Instituts für Photogrammetrie der Universität Stuttgart*, Heft 13, pp. 223–242.

Wu, J., and J. H. Chang, 1990. Unified analysis of matching and positioning with stereoscopic digital images, *International Archives of Photogrammetry and Remote Sensing*, Symposium Wuhan, Com. III, Vol. 28, Part 3, pp. 1016–1024.

Zheng, Y. J., and M. Hahn, 1990. Surface reconstruction from digital images in the presence of discontinuities, occlusions and deformations, *International Archives of Photogrammetry and Remote Sensing*, Symposium Wuhan, Kommission III, Vol. 28, Part 3, pp. 1121–1144.

(Received 17 December 1990; accepted 10 June 1991)